Jun 28th, 4:00 PM

Spillway Deflector Design Using Physical and Numerical Models

M. Politano
University of Iowa, marcela-politano@uiowa.edu

T. Lyons
University of Iowa

K. Anderson
Idaho Power Company

S. Parkinson
Idaho Power Company

L. Weber
University of Iowa

Recommended Citation

Politano, M., Lyons, T., Anderson, K., Parkinson, S., Weber, L. (2016). Spillway Deflector Design Using Physical and Numerical Models. In B. Crookston & B. Tullis (Eds.), Hydraulic Structures and Water System Management. 6th IAHR International Symposium on Hydraulic Structures, Portland, OR, 27-30 June (pp. 417-427). doi:10.15142/T3470628160853 (ISBN 978-1-884575-75-4).

6th International Symposium on Hydraulic Structures Portland, Oregon, USA, 27-30 June 2016
Hydraulic Structures and Water System Management
ISBN 978-1-884575-75-4 DOI: 10.15142/T3470628160853

Spillway Deflector Design Using Physical and Numerical Models

M. Politano[1], T. Lyons[1], K. Anderson[2], S. Parkinson[2] and L. Weber[1]
[1]IIHR – Hydroscience & Engineering
The University of Iowa
Iowa City, IA 52242
USA
[2]Idaho Power Company
P.O. Box 70
Boise, ID 83707
USA
E-mail: marcela-politano@uiowa.edu

ABSTRACT

Elevated total dissolved gas (TDG) can be a serious threat to migrating fish. Gas supersaturation downstream of a dam occurs due to bubble dissolution in deep high-pressure regions in the tailrace. TDG production depends on both air entrainment and depth of entrained bubbles. Deflectors installed at the spillway face are designed to change the regular plunging jets into surface jets, where bubbles are transported in a thin surface layer minimizing dissolution. Distinct flow conditions may, however, occur depending on the deflector geometry, spillway flowrate, and tailwater elevation. Deflectors are commonly designed based on jet regimes observed in physical and CFD models. Since bubbles are not scaled in the physical models and most commonly used CFD models do not predict the TDG field, deflector performance cannot be fully evaluated with this methodology.

This paper presents the design of spillway deflectors at Hells Canyon Dam using a 1:48 scale laboratory model and a two-phase flow model capable of predicting TDG production, dilution, and downstream mixing. The numerical model was validated against jet regimes observed in the laboratory and TDG field data. After a deflector was selected, possible fish injury due to pressure and acceleration changes near the deflector was estimated with a particle tracking technique.

Keywords: *deflectors, total dissolved gas, physical model, CFD model, supersaturation, jet regime*.

1. INTRODUCTION

Spill, considered one of the safest fish passage strategies, was historically used to enhance fish survival. However, large spill volumes can be harmful for fish since they can increase TDG, which may lead to gas bubble disease. TDG levels are usually reported relative to atmospheric pressure. Current regulation limits TDG levels to 110%. Washington and Oregon have granted waivers for the Columbia and Snake hydropower facilities to facilitate fish migration that allow 120% TDG downstream of a dam and 115% in the downstream dam's forebay when spill occurs. Hells Canyon Dam (HCD) can neither meet Idaho nor Oregon state standards for TDG during spill in excess of about 71 m^3/s. In order to meet state and federal regulations, Idaho Power Company developed a TDG study plan that includes the design of spillway deflectors (Myers et al. 1999).

Gas supersaturation occurs when bubbles are carried to deep regions where solubility is enhanced by high pressure. TDG production depends on gas volume fraction, bubble interfacial area, and bubble depth. Figure 1 shows the main TDG processes downstream of a spillway. TDG concentration depends on extremely complex processes such as air entrainment, breakup and coalescence of entrained bubbles, bubble dissolution, degasification at the free surface, and bubble and TDG transport. In addition, powerhouse flows might be attracted towards the spillway region, increasing the volume of water exposed to bubbles modifying TDG production and dilution.

One alternative to minimize TDG supersaturation is to install deflectors on the spillway face to change the regular plunging into surface jets with most of the spilling momentum tangential to the free surface (Figure 2). In this regime, bubbles are transported in a thin surface layer minimizing dissolution. Distinct flow conditions may, however, occur depending on the deflector geometry, spillway flowrate, and tailwater elevation. Deflectors are commonly designed based on the capability of producing surface jets under a wide range of spillway flowrates and tailwater elevations. Figures 1 and 2 show a schematic of the flow pattern observed downstream of spillways; deflector and spillway shape in the figures do not reflect the particular geometry of HDC.

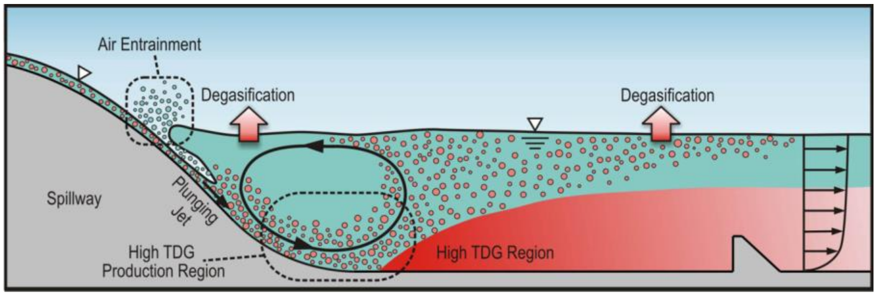

Figure 1. Air entrainment and TDG processes downstream of a spillway

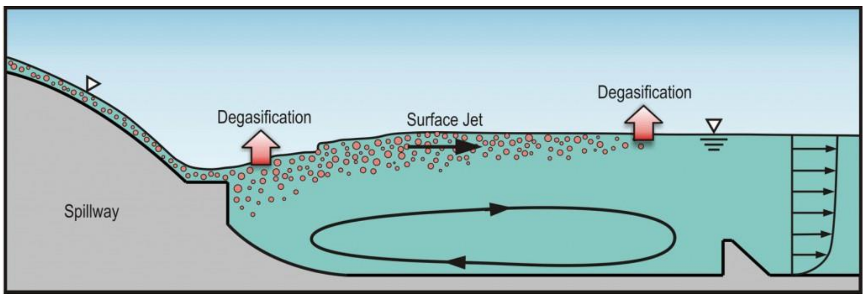

Figure 2. Surface jet in a spillway retrofitted with deflector on the spillway face

Deflector performance is usually tested in a physical model before installation in the field. Empirical models to predict TDG downstream of spillways have been developed and widely used to evaluate TDG production or refine the deflector design in several dams in the Columbia River Basin (Hibbs and Gulliver 1997, Shaw 1998, Geldert et al. 1998, Orlins and Gulliver 2000, Urban et al. 2008, Li et al. 2009, Schneider and Hamilton 2009, among others). In the past 15 years, CFD models emerged as a tool to simultaneously predict the hydrodynamics and TDG distribution downstream of dams (Weber at al. 2004, Gulliver et al. 2009, Politano et al. 2009, Feng et al. 2013). Most commonly used CFD models neglect the effect of the bubbles on the flow field and assume isotropic turbulence. Since the most important source of TDG is the gas transferred from the bubbles, a proper model for TDG prediction must account for the two-phase flow in the stilling basin and the mass transfer between bubbles and water. Moreover, bubbles modify the effective density and viscosity, changing the jet regime downstream of the deflector. Turbulence modeling also plays an important role since turbulence levels near the free surface are over-predicted by isotropic models, resulting in ineffectual prediction of spillway jet regimes (Turan et al. 2007). Advances in computer technology have made the use of three-dimensional two-phase flow modeling possible to optimize the design of spillway deflectors and complement physical models. In this paper, various configurations of deflectors in the sluiceways of HCD were evaluated, and a deflector design was selected using physical and two-phase flow models. Fish injury was then estimated based on acceleration and strain rate down the sluiceway.

2. HELLS CANYON DAM

HCD is located at river mile 247.7 on the Snake River. Figure 3 shows the dam structures and tailrace bathymetry. The dam comprises three upper crest gates, two lower level or sluice gates, nappe deflectors, left and right training walls, three powerhouse units, non-overflow sections, a left bank guidewall, and a diversion tunnel outlet. Data from multi-beam and single beam bathymetry and photogrammetry supplied by Idaho Power were used to generate the riverbed downstream of the dam.

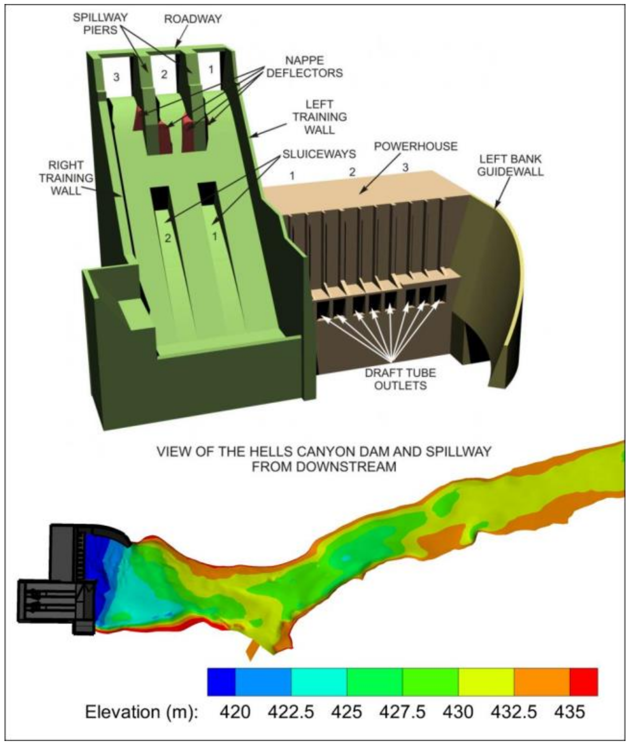

Figure 3. Hells Canyon Dam

3. PHYSICAL MODEL

Since gravitational forces are predominant, Froude similarity was used for the physical model (White 1999). A 1:48 model scale was selected based on discernable flow characteristics, available laboratory space, and construction cost. Scaling ratios based on Froude similarity for the flowrate, Reynolds number, and Weber number are 1:15963, 1:332.6, and 1:2304, respectively. Smaller levels of turbulence and smaller and larger bubbles (in dimensionless terms) in the physical model prevent the capture of bubble behavior and TDG production. However, although the Reynolds-number similarity is violated, conditions simulated in the laboratory corresponded to fully turbulent flow, and the model is expected to reproduce the spillway jet regime and general flow pattern in the tailrace. The original physical model recreated the entire spillway section and was used to develop the deflector performance curves. This sectional model consisted of a large head tank, a spillway section, and an open-channel flume. A Plexiglas wall as one side of the downstream flume permitted flow visualization for the various deflector designs. The model was later modified for investigation of potential erosion impacts and three-dimensional flow characteristics. The spillway section, powerhouse units, left and right bank training walls, forebay area, and about 1 km of downstream tailrace were included in the model

Potential for erosion was evaluated only with the physical model. Deflectors significantly changed the tailrace flow pattern and increased tailrace erosion potential at flowrates above 425 m^3/s per sluiceway bay. Model observations indicated that spill operations should change after deflector installation to minimize erosion. For total spill flowrates of 850 m^3/s or less, only sluiceways should be opened evenly. At spill flowrates between 850 and 5600 m^3/s, only upper crest gates should be opened evenly. Above 5600 m^3/s, both fully opened crest gates and evenly opened sluiceway gates should be used.

4. TWO-PHASE FLOW MODEL

The study area used for the CFD model includes about 11.4 km of the Snake River, beginning at HCD and extending downstream to just below to Wild Sheep rapids. The model is based in the commercial CFD code ANSYS FLUENT. The free-surface shape in the 300 m downstream of the dam was obtained with a VOF method assuming a negligible effect from the bubbles. Mike 11 was used to predict the water elevation in the river downstream.

A rigid-lid grid conformal to the predicted free surface was created, and a slip mixture two-phase flow model with attenuation of normal velocity fluctuation at the free surface was used for the hydrodynamics and TDG prediction. The model accounts for buoyancy, pressure, drag, and turbulent dispersion forces. A transport equation for the bubble number density was used to predict the local bubble size, which can change with dissolution and pressure. The model uses a Reynolds Stress Model to provide anisotropic turbulence closure. In order to capture the turbulence structure and attraction of powerhouse flows by spillway jets, zero normal fluctuations at the free surface are enforced. A modified bubble-induced turbulence term is used to account for suppression and production of turbulence by the bubbles. The TDG field is calculated with a two-phase scalar transport equation in which the source is the bubble/liquid mass transfer, function of the gas volume fraction, and bubble size. Details of the mathematical model, model limitations, numerical schemes, and implementation using User Defined Functions in FLUENT are presented in Politano et al. (2009).

Fish mechanical injury due to spillway deflectors was analyzed using a particle tracking technique. The history of accelerations and strain rate on particles released from the sluiceways gates was recorded and linked to injury values reported in the literature. Fish are assumed to be passive, neutrally buoyant particles with no behavioral responses, which is expected to be valid at the high velocity found in the sluiceway.

5. DEFLECTOR PERFORMANCE CURVES

Deflector design at HCD is challenging due to the unique project characteristics such as high head, upper nappe deflectors, lower level sluiceways, and a short, deep stilling basin. Initial laboratory tests demonstrated that upper nappe deflectors would be problematic since the flow is deflected away from the concrete spillway surface. Dam operation flexibility could be maintained if an acceptable deflector design could be developed for the lower level sluiceways. A balance between energy dissipation and bubble entrainment must be achieved for acceptable flow deflector design. The lower level sluiceways could then be operated when TDG levels are important, and the upper spillway gates could be operated for high spill discharges when energy dissipation and dam safety become important.

The jet regime depends on the spillway discharge per bay and tailwater elevation. Figure 4 shows different spillway regimes observed in the laboratory. Figure 4 shows the jet regime for a spillway flowrate of 141.5 m^3/s using a deflector 4.88 m long with 5° lip angle at an elevation 448 m. A surface jump occurs during high tailwater elevations. A hydraulic roller forms above the jet, aerating the downstream water surface with potential of TDG production (Figure 4a). The most efficient regime to prevent TDG production is the surface jet (Figure 4b) in which the jet remains tangential to the free surface, minimizing the bubble transport to depth and TDG production. In the vented surface jet (Figure 4c), the jet is still surface oriented but the nappe begins to intermittently aerate. At low tailwater elevations, water flowing over the spillway plunges deep into the stilling basin, resulting in a plunging regime with the highest TDG production (Figure 4d).

Primary flow deflector design components include elevation, length, transition radius, and lip angle. Deflector elevation must remain below the tailwater level to prevent vented surface and plunging flows and high enough to keep performance within the surface jet flow regime for high tailwater. Deflectors must be long enough to deflect flow but short enough to minimize construction cost. Cavitation is also a factor of concern in flow deflector length. Sluiceway bay deflectors at HCD could cause cavitation problems if they extend beyond the spillway face. The transition radius is the radius of an arc connecting the sluiceway face to the horizontal deflector face. A 4.5 m transition radius was used initially to minimize fish injury. Three positive lip angles were then examined over the course of the model.

A performance curve shows flow regimes regions for different sluiceway unit discharges and tailwater elevations for a given deflector geometry. These plots are used to compare deflector designs and to optimize operating conditions once a deflected is selected. The curve was created in the physical model first setting a given discharge in each sluiceway. After the forebay was stabilized, which took approximately 15 minutes, the tailwater elevation was set to approximately 450 m, providing deep deflector submergence. The corresponding flow regime for this tailwater was observed and recorded. The tailwater was gradually lowered until a flow regime change was observed. The discharge, tailwater elevation, and flow regime were then recorded. This procedure was repeated until plunging flow regime was observed. This process was implemented for different flows per sluiceway bay for various deflector designs (length from 4.3 to 5.57 m, elevation from 446.2 to 447.4 m, lip angle: 0, 10 and 15 degrees). Figure 5 shows the performance curve for a deflector 4.87 m long with a 5° lip angle set at elevation 447.4 m. This deflector demonstrated the highest potential for minimizing TDG of all tested deflectors in the laboratory,.

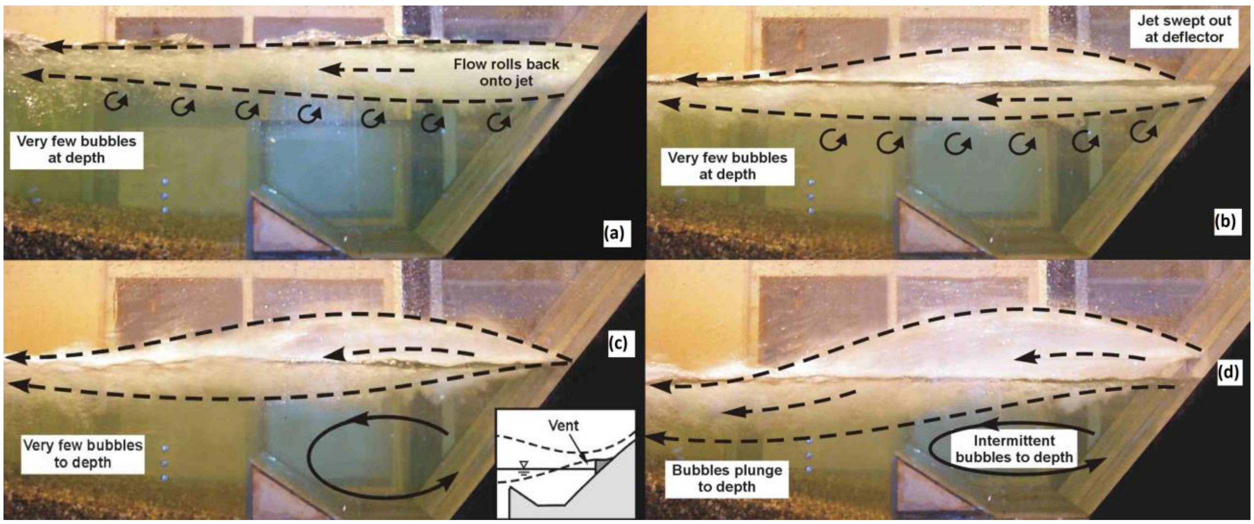

Figure 4. Jet regimes observed in the laboratory model. Surface jump (a), surface jet (b), vented surface jet (c) and plunging flow (d)

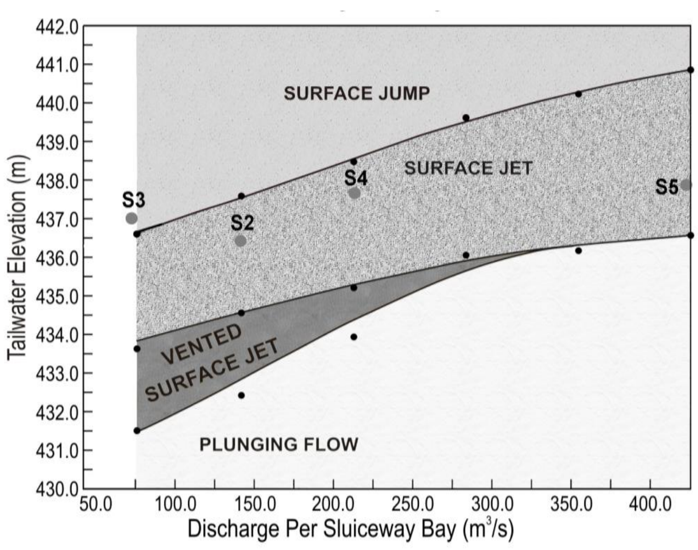

Figure 5. Deflector performance curve

Four numerical simulations were performed for the deflector selected in the laboratory to compare predicted jet regimes with those observed in the physical model. For unit discharges of about 100 m^3/s, the model predicted a surface jet similar to that observed in the laboratory (Figure 6). Also consistent with the laboratory results, a surface jump with waves at the impact region was predicted at the lowest discharge per bay (simulation S3). Figure 6 shows the surface jump predicted in slices through the middle of the low-level sluice gates SG1 and SG2 for simulation S3. White lines represent the free surface location. Velocity vectors above the free surface show air velocity. Note that 3D effects predicted with the numerical model are not captured by a sectional model. Lateral powerhouse flows reduce the performance of the deflector. This effect is more important at low spillway flows, and it was observed in both the numerical model and laboratory model with the powerhouse and tailrace included.

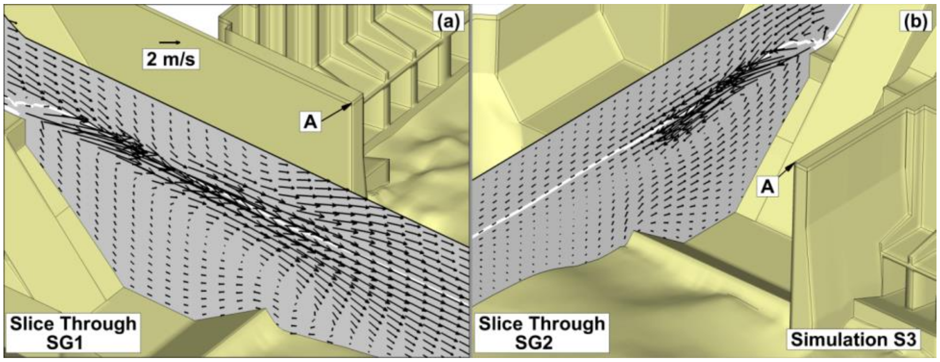

Figure 6. Predicted jet regimes for simulation S3. Velocity vectors in a slide passing through SG1 (a) and SG2 (b)

6. CALIBRATION AND VALIDATION OF TDG MODEL

Inputs of the two-phase model are bubble diameter and gas volume fraction at the spillway inflows, representing the air entrainment. Different bubble sizes and gas volume fractions were used to determine the parameters that produced the least error between modeled TDG and field data collected on May 21, 1998 and May 4, 2006. Three gas volume fractions, α = 0.03, 0.04, and 0.045, and two bubble diameters, 0.5, and 0.8 mm, were tested. The parameters that produced the smallest difference with the field data were α = 0.03 and bubble diameter 0.8 mm. The entrained gas volume fraction and bubble size distribution are expected to change with flow conditions and spillway geometry. Unfortunately, TDG data at HCD were insufficient to obtain model parameters for different spillway flow regimes. However, the values obtained for HCD are comparable to those used at other hydropower projects with and without deflectors (Politano et al. 2009, Politano et al. 2011). Table 1 shows the percent of saturation of TDG measured in the field at the forebay and tailrace as well as the results of the model. The model matched the results of the field measurements with an error smaller than +/- 3%.

Table 1. Measured and predicted TDG concentrations

	TDG Saturation								
	Field Data			Model				Error %	
	Forebay	RM 246.87	RM 246.38	Forebay	RM 246.87 Average	RM 246.87 Near Oregon	RM 246.38 Average	RM 246.87	RM 246.38
May 21, 1998	1.170	1.268		1.170	1.358	1.280		0.950	
May 4, 2006	1.224	1.321	1.366	1.224	1.349	1.304	1.329	-1.290	-2.710

Figures 7a and 7b show gas volume fraction contours predicted by the model in vertical slices on May 21, 1998 and May 4, 2006. Bubbles are transported to deep regions in the tailrace due to the plunging jets created by spillway and sluiceway flows. High velocity water plunges deep into the stilling basin, creating a vertical recirculation upstream of the roller bucket. This recirculation moves bubbles up near the free surface to regions of low pressure with lower dissolution rate. Bubbles are present within 200 m downstream of the dam. The percentage of spill on May 21, 1998 and May 4, 2006 were 54% and 49%, respectively, and river flowrates were comparable. Larger spills favor plunging, resulting in a slightly higher concentration of bubbles at depth on May 4, 2006. According to the model, surface spill flows move towards the powerhouse region, transporting some bubbles to this region. This phenomenon is more pronounced for smaller spill flowrates. The TDG model assumes that no air is entrained with turbine flows, which explains the low gas volume fraction close to the powerhouse. TDG isosurfaces presented in

Figures 7(c) and 7(d) display a similar TDG field for May 21, 1998 and May 4, 2006. Maximum TDG values are found within 100 m from the dam as a consequence of bubble dissolution. High TDG concentrations, of the order of 180%, are predicted near the stilling basin.

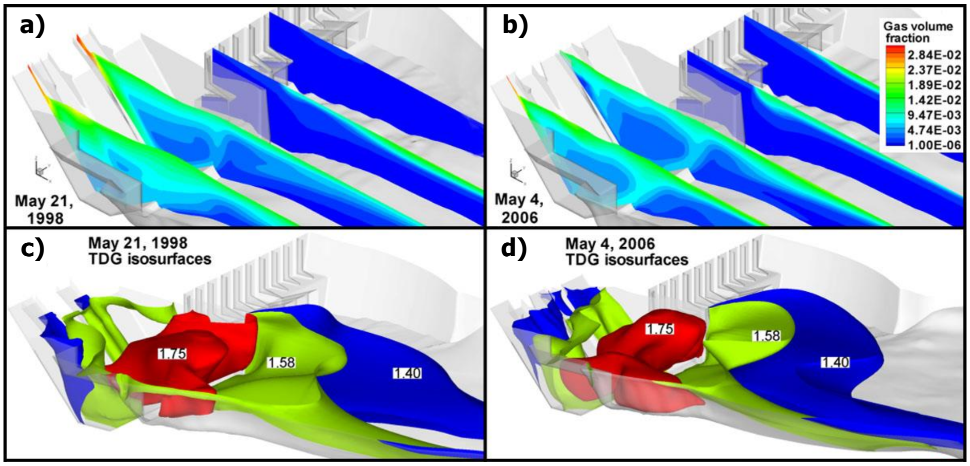

Figure 7. TDG model results. May 21, 1998 (left) and May 4, 2006 (right). Slices with gas volume fraction contours (a) and (b) and TDG isosurfaces (c) and (d)

7. HYDRODYNAMICS AND TDG CONCENTRATION

The flow pattern obtained with the numerical model compared qualitatively well with that observed in the physical model. Figure 8 shows the simulated and observed free surface for the selected deflector at a river flowrate of 1274 m^3/s. Sluice surface jets created by deflectors generate a local depression in the water elevation near the spillway that depends on the flowrate and tailwater elevation. Spillway flow travels through the pool alongside the powerhouse wall, creating one clockwise recirculation near the right bank training wall. A counterclockwise recirculation near the fish trap is also predicted in the simulations with moderated and elevated spill flowrates. For this simulation, surface jets generate waves near the spillway with amplitude of approximately 0.60 m. The wave amplitude is significantly smaller than predicted for plunging flows without deflectors, but the waves propagate farther downstream impacting a larger region of the tailrace. Comparisons at additional flowrates are found in Politano and Carbone (2012).

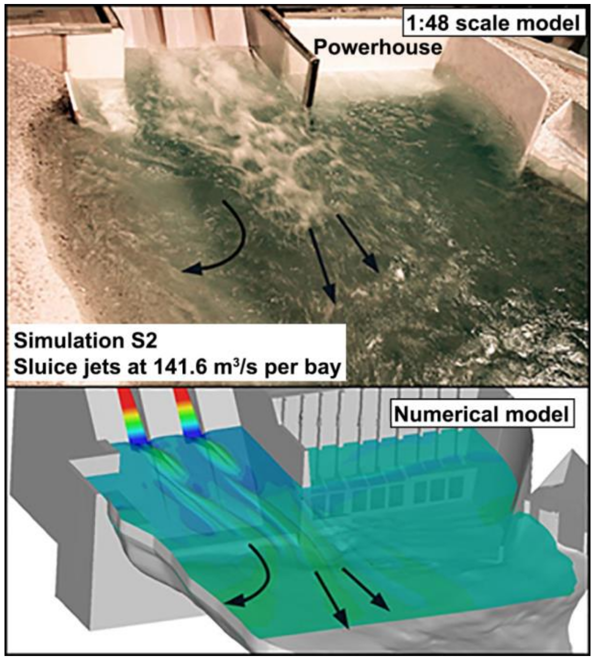

Figure 8. Flow pattern in the tailrace observed in the physical model (top) and predicted with the model (bottom)

Eight additional numerical simulations (SI to SVIII) were performed to test different deflector geometries for river flowrates of 707 (odd number simulations) and 1274 m^3/s (even number simulations). These simulations assumed a constant flow of 212.4 m^3/s passing through each of the sluiceways and no flow through the upper spillway gates. Two simulations with the highest average flow that occurs for a period of seven days in a once in ten years period (7Q10 flow) were also carried out to estimate possible fish injury due to inclusion of deflectors.

Streamlines colored by TDG for different deflector geometries are shown in Figure 9. Simulations SI and SII are for the deflector selected in the physical model, SIII and SIV a deflector 0.3 m higher, SV and SVI a deflector 0.3 m shorter, and SVII and SVIII comprise a 7.6 m curvature radius. Figures 9(a-d) are for a river flowrate of 707 m^3/s and Figure 9(e-h) are for river flows of 1274 m^3/s. An important recirculating zone near the left bank, which might affect the efficiency of the fish trap, is predicted by the simulations with a river flow of 707 m^3/s. This recirculation is created by attraction of ambient water beneath the surface jets created by deflectors. According to Turan et al. (2007), this phenomenon can be explained by acceleration of the surrounding fluid as the jet decelerates, surface currents, and the Coanda effect. For simulations with a river flow of 1274 m^3/s, this flow patterns is observed only in simulation SIV, which has the deflector placed at the highest elevation and is able to maintain a surface jet for higher tailwater elevations. Simulations with a river flow of 1274 m^3/s have three times more powerhouse flow than those with a total river flow of 707 m^3/s, and, therefore, downstream TDG dilution is more important. According to the simulations, the shorter deflector produces a weaker surface jet and favors some plunging downstream. Note that, as an additional factor, a weaker surface jet entrains less water from the powerhouse region, which results in more bubbles falling deeper and earlier in the tailrace the highest values of TDG. Maximum values of TDG production are predicted for the simulation with the greatest transition radius. However, this case also predicts higher degasification near the free surface, and the resulting TDG concentration is smaller than the case with shorter deflector.

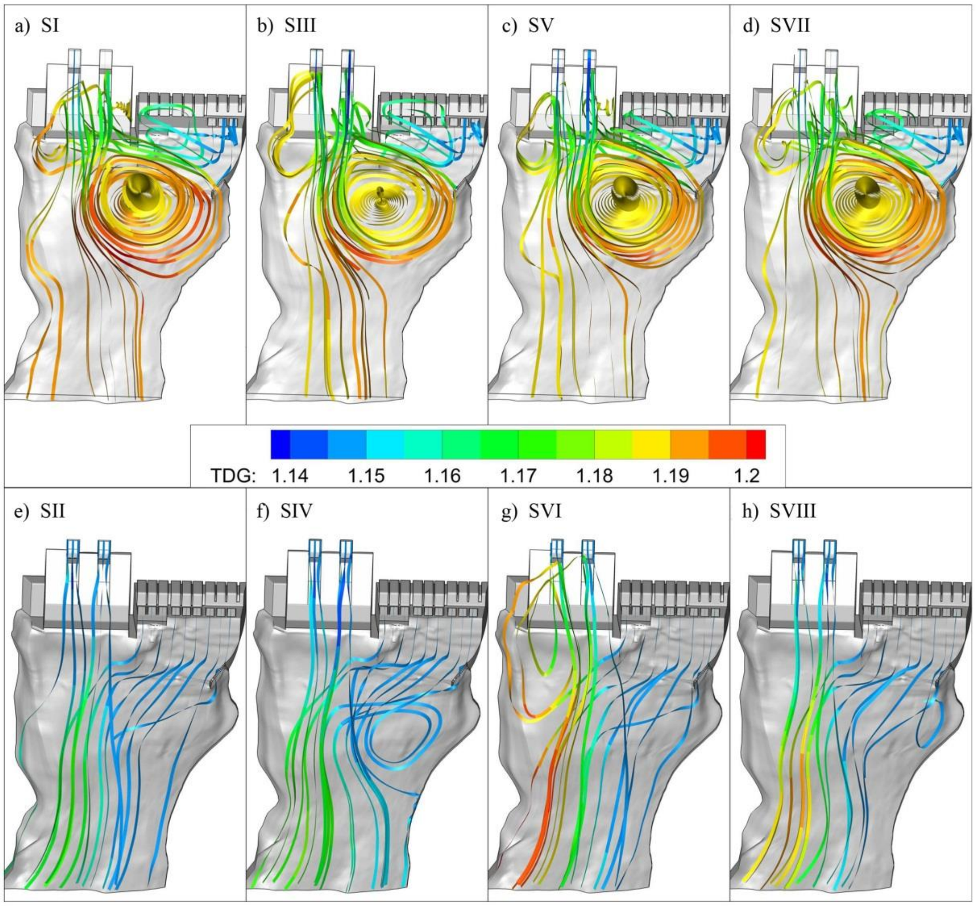

Figure 9. Streamlines colored by TDG for 707 m^3/s (top) and 1274 m^3/s (bottom)

8. FISH INJURY

Results from the VOF model for a 7Q10 flow with and without deflectors were used to analyze fish injury. For each operating condition, 6000 particles were released. Figure 10 shows values of flow acceleration and strain rate when the deflector is included (averaged every 0.5 m). Particles moving downstream over the sluiceways are exposed to a space-averaged maximum acceleration of 165 m/s^2. Maximum values of space-averaged acceleration coincide with changes in flow direction due to inclusion of the deflector in the sluiceway. When particles move over the spillway without deflectors, the space-averaged maximum acceleration is 76.2 m/s^2. In this case, the maximum acceleration occurs when flow plunges the basin pool.

The averages of the particle maximum accelerations for the cases with and without deflectors are 180.6 and 170.2 m/s^2, respectively. According to Deng et al. (2005), maximum accelerations experienced by the particles in the simulation with deflector have, on average, probabilities of 0.095 and 0.028 of causing minor and major injuries in fish, respectively. The probabilities of minor and major injuries without the deflector are 0.088 and 0.026. It is important to note that the experiment presented in Deng et al. (2005) introduced fish into a submerged jet with different water velocities. Fish injuries reported by this experiment could also be caused by the elevated shear present at the moment fish were introduced into the jet. Fish passing over the sluiceway and spillway are expected to be accelerated with the flow, and, thus, they may not be exposed to the same levels of shear as fish in the experiment. The average of the particle maximum strain rates are 20.3 and 28.6 s^{-1} for the simulations with and without the deflector, respectively. Maximum values recorded for a single particle are 47.6 and 210.8 s^{-1}, respectively. These values of strain rate are below the value of 360 s^{-1} reported by Foust et al. (2010) as detrimental to fish life.

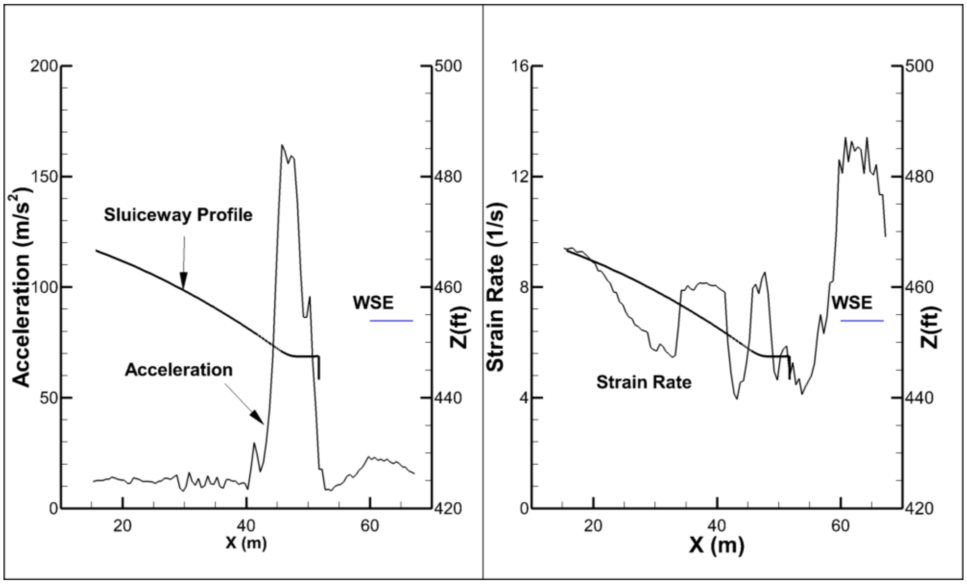

Figure 10. Space-averaged acceleration (left) and strain rate (right) for 7Q10 flow

9. CONCLUSIONS

Spillway deflectors that meet the specified design goals to reduce TDG concentration downstream of HCD were recommended using a 1:48 laboratory scale and two-phase flow models. Numerical model results agreed with observations at the physical model. A 4.87-m deflector with a 5° lip angle at elevation 447.4 m has the highest potential to minimize TDG and avoid negative flow patterns that could affect the operation of the fish trap. The recommended sluiceway deflectors retain operational flexibility to pass spill flows larger than 849.5 m^3/s through the upper spill gates while dissipating enough energy to maintain the structural integrity of the dam. The numerical model was used to further exploration of deflector performance, flow deflector effects on general flow patterns in the tailrace, and possible fish injury. Results show that with the recommended deflector, a negligible amount of bubbles is transported to depth and TDG field meet the standards for all tested conditions. Particle tracking simulations were performed to evaluate possible fish injury. On average, particles moving over the sluiceways with deflectors were exposed to higher accelerations than particles moving over the spillways. According to the values presented in Deng et al. (2005) and the results of the model, fish passing downstream of HCD are not likely to suffer severe mechanical injuries.

10. REFERENCES

Deng, Z., Guensch, G,R., McKinstry, C.A., Mueller, R.P., Dauble, D.D., and Richmond M.C. (2005). “Evaluation of fish-injury mechanisms during exposure to turbulent shear flow.” Can. J. of Fisheries and Aquatic Sciences, 62(7): 1513-1522.

Feng, J., Li R., Yang, H., and Li, J. (2013). “A laterally averaged two-dimensional simulation of unsteady supersaturated total dissolved gas in deep reservoir.” J. of Hydrodynamics 25: 396-403.Foust, J.M., Coulson, S., Hecker, G.E., Allen, G.S., and Dixon D.A. (2010). “Design considerations for the Alden fish friendly hydro turbine”. Proc. Hydrovision International, Charlotte, NC, USA

Geldert, D.A., Gulliver, J.S., and Wilhelms, S.C. (1998). “Modeling dissolved gas supersaturation below spillway plunge pools.” J. Hyd. Eng., 124(5): 513-521.

Gulliver, J.S., Groeneveld, J., and Paul, G.E. (2009). “Prediction of total dissolved gas below the Cabinet Gorge Spillway.” Proceedings, XXXIII Congress of IAHR, August 9–14, 2009, Vancouver, B.C.

Hibbs, D.E., and Gulliver, J.S. (1997). "Prediction of effective saturation concentration at spillway plunge pools." J. Hyd. Eng., 123(11): 940-949.

Li, R., Li, J., Li K., Deng, Y., and Feng, J. (2009). "Prediction for supersaturated total dissolved gas in high-dam hydropower projects." Science in China Series E: Technological Sciences, 52(12), 3661-3667.

Myers, Ralph, Stan Pierce, and Mark Stute. (1999) "Hells Canyon Complex Total Dissolved Gas Study." Project Progress Report. Idaho Power Company.

Orlins, J.J., and Gulliver J.S. (2000). "Dissolved gas supersaturation downstream of a spillway II: computational model." J. Hyd. Res., 38(2): 151-159.

Politano, M., Carrica, P., and Weber, L. (2009). "A multiphase model for the hydrodynamics and total dissolved gas in tailraces." Int. J. Multiphase Flow, 35(11): 1036-1050.

Politano, M. S., Arenas Amado A., Bickford, S., Murauskas J., and Hay D. (2011). "Investigation into the total dissolved gas dynamics of Wells Dam using a two-phase flow model." J. Hydraulic Engineering, 137(10): 1257-1268.

Politano M. and Carbone M. 2012. Numerical model in the tailrace of Hells Canyon Dam. Phase V: Deflector optimization. IIHR LDR No 378.

Schneider, M. and Hamilton, L. (2009). "SYSTDG manual". U.S. Army Corps of Engineers Report.

Shaw, P. (1998). "Gas generation equations for CRiSP 1.6". University of Washington, Seattle, Washington. <http://www.cbr.washington.edu/d_gas/tdg_manual.pdf.> (Aug. 2015).

Turan, C., Politano, M.S., Carrica, P.M., and Weber, L. (2007). "Water entrainment due to spillway surface jets." Int. J. Computational Fluid Dynamics, 21 (3-4): 137-153. Urban, A.L., Gulliver, J.S., and Johnson, D.W. (2008). "Modelling total dissolved gas concentration downstream of spillways." J. Hyd. Eng. 134: 550-561.

Weber, L., Huang, H., Lai, Y., and McCoy, A. (2004). "Modeling total dissolved gas production and transport downstream of spillways: three-dimensional development and applications." J. River Basin Management 109: 157-167.

White, Frank M. (1999) Fluid Mechanics. 4th ed. Boston: WCW/McGraw-Hill.